Wireless Communication project

Conception of a complete OFDM communication channel

Moulin Léo
Rouvroy Alexis
Schoone Rudy

2017-2018

Table des matières

1 Introduction

This project consists in designing and implementing an OFDM wireless communication in Matlab. In this report we will resume the theoriticals notions that we use in our project, explain the implementation of our wireless communication and present the results.

2 SISO Communication

2.1 Channel model

To model the channel we will firstly model its PDP, and afterwards model the transfer function of the channel.

2.1.1 Power Delay Profile (PDP)

The PDP represents the spread in time of the power received by the antenna due to the multipaths components of the signal. Some components have more travel time and are consequently late, their transmitted power will then be delayed.
To model the PDP we will use an exponential function, this choice is motivated by the fact that the PDP decreases quickly : more a multipath component is late, more it experiences diffusion, reflection, etc. and is thus attenuated.

We start by downloading the data of frequency responses for each position of the receiver and compute the impulse response by using the inverse fast Fourier transform. After this, we take the 50 first values of the impulse response after its maximum, then we have just to sum the impulse responses of each position as given by the formula :

$$PDP = \frac{1}{N} \sum_{i=1}^{N} |h_i(n)|^2 \tag{1}$$

To observe the influence on the PDP of a smaller bandwidth, we constructed two other frequency responses (LOS & NLOS). We applied a rectangular window on the frequency responses to obtain a bandwidth 10 times smaller and we downsampled the impulse responses by the same factor.

We must now compute the parameter of our model that is the "delay spread" by the formulas :

$$\tau_m = \frac{1}{P_T} \int_0^\infty \tau P(\tau) d\tau \tag{2}$$

$$\sigma_\tau = \sqrt{\frac{1}{P_T} \int_0^\infty \tau^2 P(\tau) d\tau - \tau_m} \tag{3}$$

You can see the comparison between the models and the measurements in the figure 1.

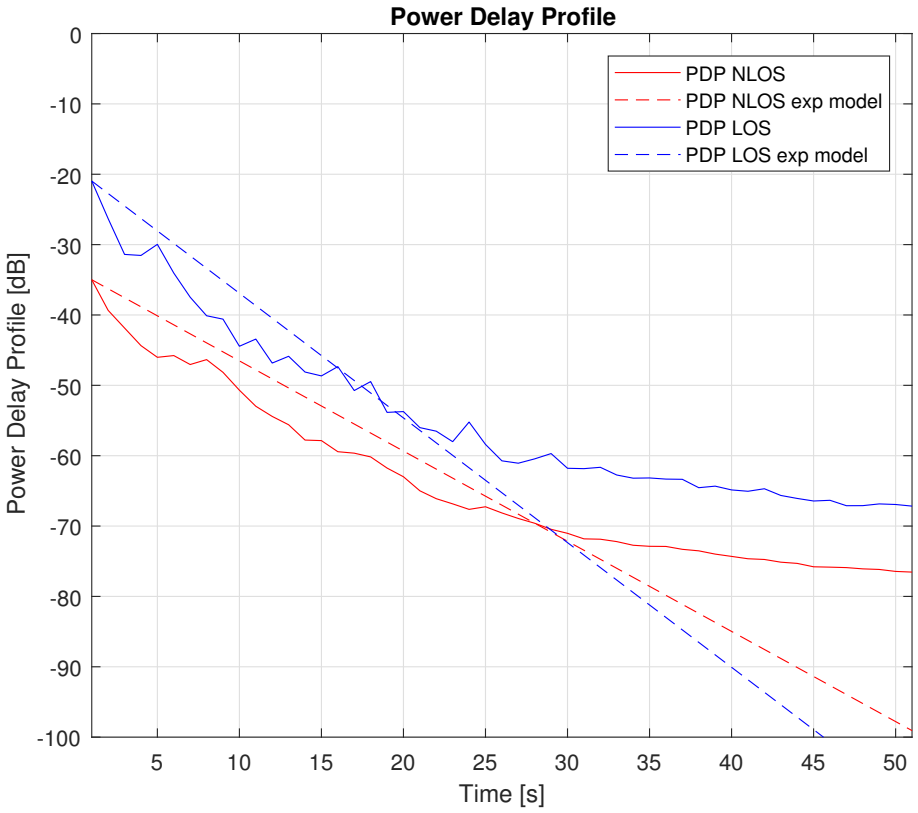

FIGURE 1 – Modeled and measured PDP

We can make some observations about these graphs :

— The first one is that there is a gap between the models and the measurements at the end of the graphs. This is probably due to the modelization by an exponential function.
— The second one is that in the case of a narrowband, the delay is about 2.5 times smaller

To compute the coherence bandwidth we applied the following formula :

$$\Delta f_c = \frac{1}{2\pi\sigma_\tau} \tag{4}$$

2.1.2 Statistical model

To calculate the transfer function of the channel, the first inclination is to do it analytically by summing all the components. For the narrowband case we applied the following formula :

$$h = \sum_{i=0}^{N-1} a_i e^{j\Phi_i} e^{-j\bar{\beta}_i.\bar{r}} \tag{5}$$

and in the wideband case :

$$\tilde{h}(n) = \sum_{i=0}^{N-1} A_i e^{j\Phi_i} e^{-j\bar{\beta}_i.\bar{r}} \delta(n\Delta\tau - \tau_i) \tag{6}$$

But these formulas need a knowledge of both the phase and amplitude of each MPC. To compute

these parameters we need to know precisely all the interactions between the waves and the interacting objects. In practice this is not possible and we choose to use a statistical model of the channel. We model the transfer function by a random function :

$$h = \sqrt{\frac{K}{K+1}} e^{j\Phi_0} + \sqrt{\frac{1}{K+1}} A e^{j\Phi} \tag{7}$$

Where :

- K is the Rician factor, it represents the ratio between the power of the direct path ans the other scattered paths.
- A has a Rayleigh distribution
- Φ has an uniform distribution

The direct path is the fastest of all and the its power is the first to faint. It implies that the K will decrease with the delay as we can see in the figure 2

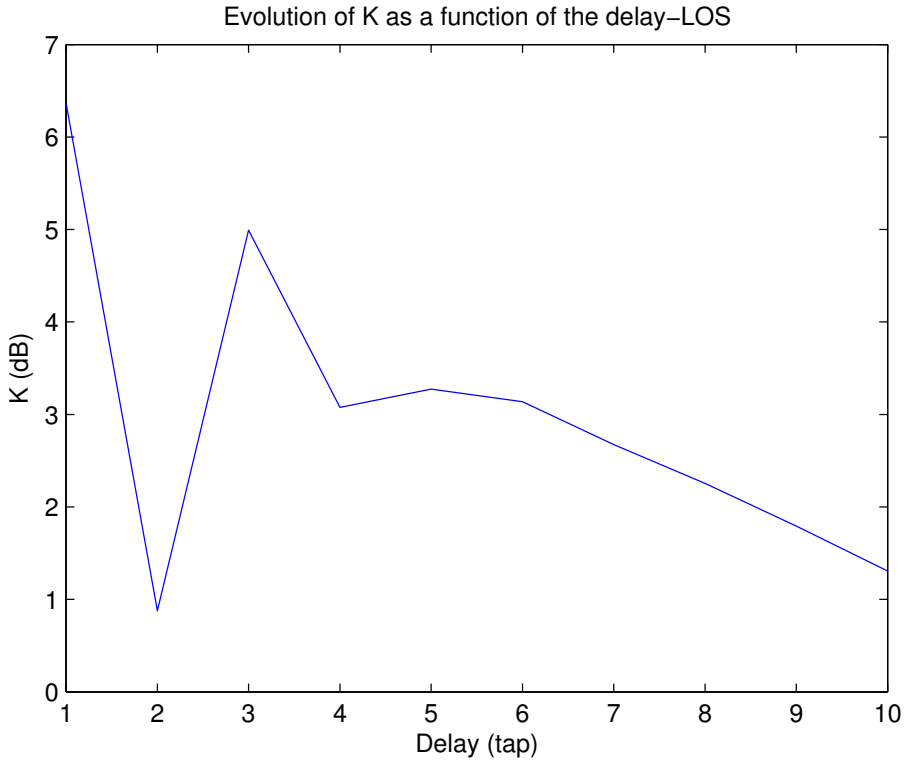

FIGURE 2 – Rice factor in function of the delay

For the wideband case the model is :

$$\tilde{h}(n) = \sum_{i=0}^{M} A_i e^{j\Phi_i} \delta(\tau - \tau_i) \tag{8}$$

Where A_i follows a Rice or Rayleigh distribution.
You can see below, in figure 3, an example of transfer function that we achieved with this method.

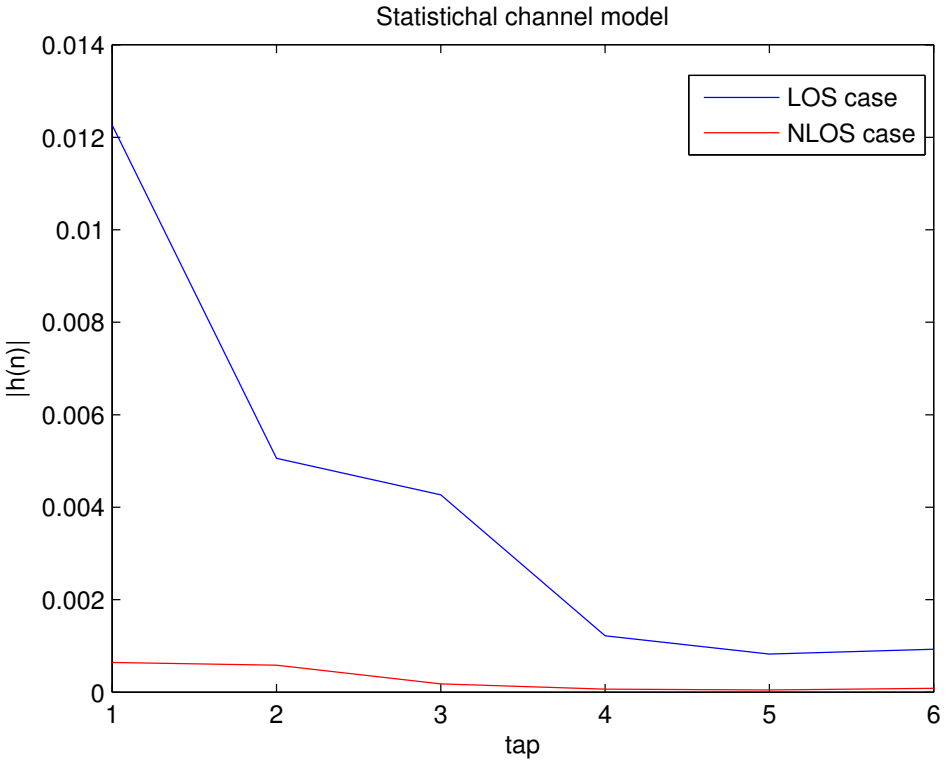

FIGURE 3 – Statistical channel model

2.2 Channel equalization

In this section, the orthogonal frequency-division multiplexing (OFDM) is implemented. The principle of OFDM is to encode the data on orthogonal narrowband sub-carriers. The wideband channel is thus divided into a a number of parallel narrowband frequency-flat sub-channel. OFDM has the advantage of a simplified channel equalization using multiple narrowband signals rather than one wideband signal. Each narrowband frequency sub-channel can be equalized quite easily by simple scalar multiplication in the frequency domain.

The sub-carriers are created as depicted on figure 4. First, there is a QAM modulation defined in the frequency domain. These symbols go through a serial to parallel (S/P) converter. The N point blocks from the converter are brought to the time domain by taking the inverse fast fourier transform (IFFT). Before reconverting it into a stream signal, a cyclic prefix is added to each block to assure the orthogonality among the sub-carrier and isolates the different OFDM block from each other. At the reception, the inverse operation are done. The signal go through a serial to parallel converter, then the cyclic prefix are taken down, the fast Fourier transform is applied, the reconversion into a stream of symbols and the demapping to get back the bits message.

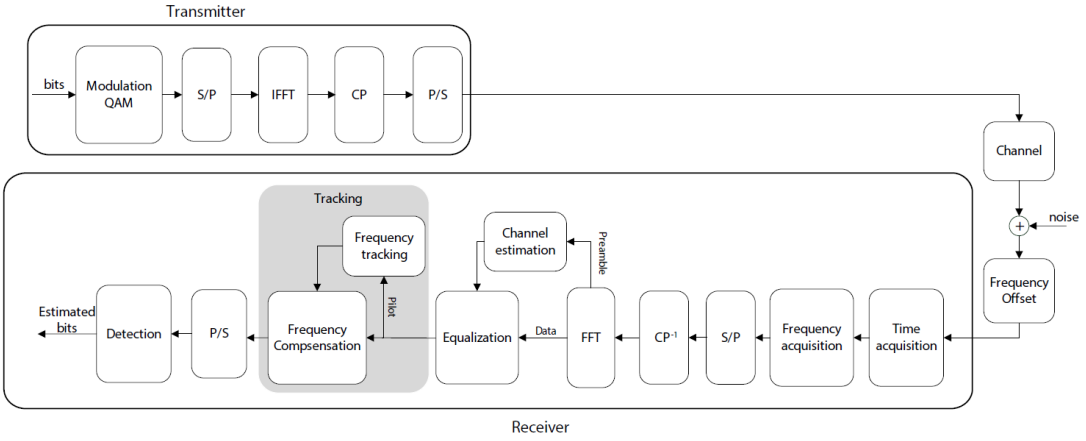

FIGURE 4 – OFDM communication system

This cyclic prefix (CP) consist in repeating the lasts symbols of each data block, and must be larger that the channel impulse response to avoid any interferences. This multiplexing method allows to facilitate the equalization of the channel at the reception using a simple scalar multiplication instead of a time domain convolution :

$$y(n) = h(n) * s(n) => Y(k) = H(k)S(k) \tag{9}$$

But, this holds only if the signal $s(n)$ is periodic which is the case thanks to the cyclic prefix. Indeed, as the CP is a simple copy of the end of the OFDM block, the linear convolution can be seen as a circular convolution, there is an illusion of periodicity.

The other advantage of using a cyclic prefix, is to avoid any interferences between blocks. Indeed, when the convolution is applied, the channel impulse response will slide over the received signal and the output will depend on a certain number of previous samples (depending on the size of the channel impulse response). Without the use of a prefix and without noise, the received symbol can be observed on Figure 5(a).

By adding a cyclic prefix, the convolution window will be entirely located in the cyclic prefix, and any interferences between blocks will be avoided, as it can be seen on Figure 5(b). Of course, this works only if the CP length is bigger than the channel impulse response length.

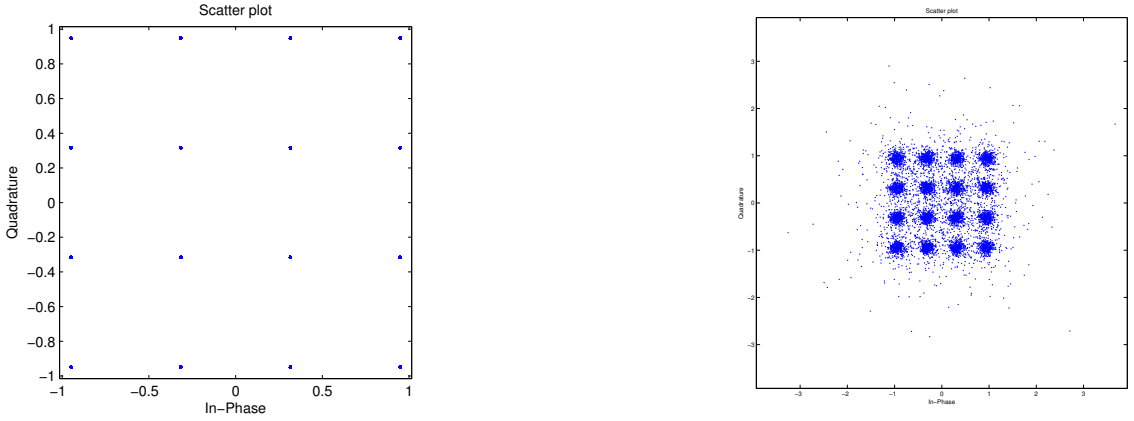

FIGURE 5 – Transmitted symbols with a sufficient CP length (a) without CP (b)

But, the communication performance is limited by Additive White Gaussian Noise (AWGN) that will corrupt the received signal. The noise being white, its power density N_0 is constant and independent of the frequency and the noise is additive, so it will be directly added to the signal. The bit error rate (BER) is assessed for (E_b/N_0) varying from -5 dB to 25 dB. The results obtained are consistent, the BER decreases as (E_b/N_0) increases, as it can be seen on Figure 6.

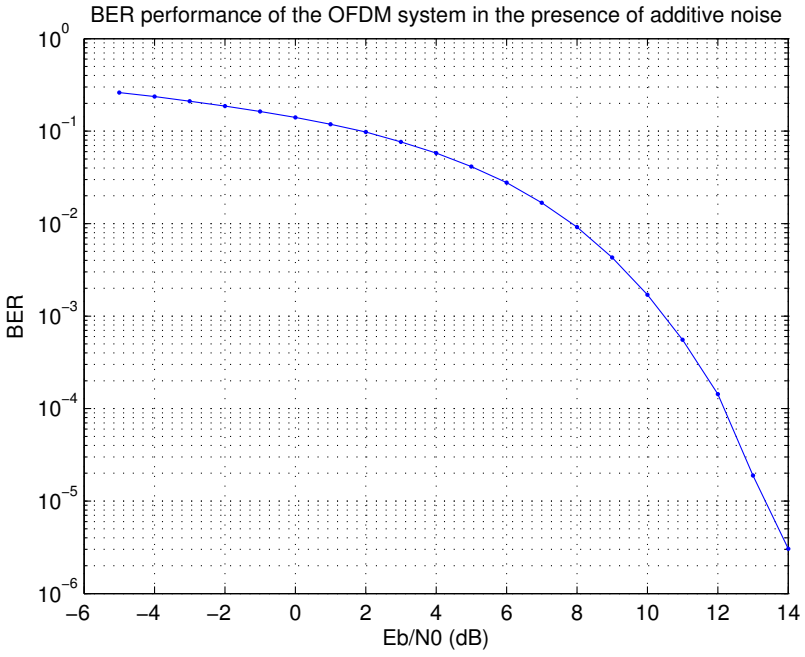

FIGURE 6 – BER performance of the OFDM system in the presence of additive noise

The next step is to assess the impact of the channel model built previously. This is done by convolving the channel with the transmitted signal and then adding the noise :

$$r(n) = h(n) * s(n) + w(n) \tag{10}$$

The channel equalization at the reception is done, after the reconversion in the frequency domain and for now by considering that the channel is known by the receiver. The performances in the LOS and NLOS scenario have been compared with the previous BER and the result is shown on Figure 7

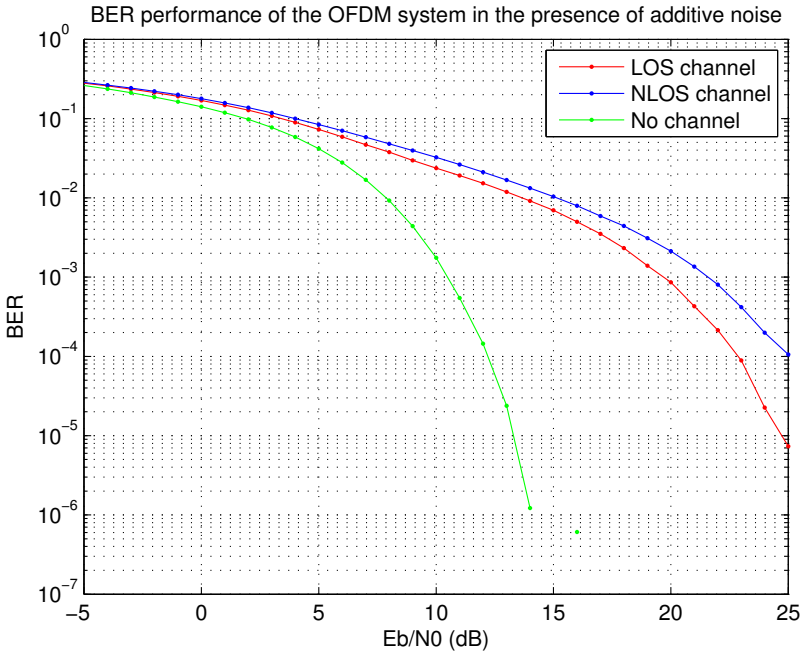

FIGURE 7 – BER performance in the LOS and NLOS scenario

As said previously, the length of the cyclic prefix needs to be larger than the channel impulse response in order to avoid inter symbol interferences. But it is not the only source of ISI, the multipath effect, can also be the cause as one signal can interfere with another. Thus, the delay spread, needs to be way smaller than the symbol duration.

2.3 Channel estimation

The next section consists of the implementation of the channel estimation. 2 known pilot symbols, consisting of -1 and +1 are added in frequency domain at the start of the frame.

The channel transfer function is estimated by dividing the frequency response of the spectrum of the received preamble symbol by the spectrum of the transmitted symbol.

$$\hat{H}(k) = \frac{R'(k)}{S'(k)} = H(k) + \frac{W(k)}{S'(k)} \tag{11}$$

The accuracy of the channel estimation is evaluated by calculating the Normalized Mean Square Error (NMSE) at different SNR levels.

$$NMSE = \frac{\sum_k |\hat{H}(k) - H(k)|^2}{\sum_k |H(k)|^2} \tag{12}$$

Figure 8 shows the advantage of using 2 preambles and taking their average. It reduces the effect of the noise. Using only one preamble for the channel estimation gives a lower accuracy.

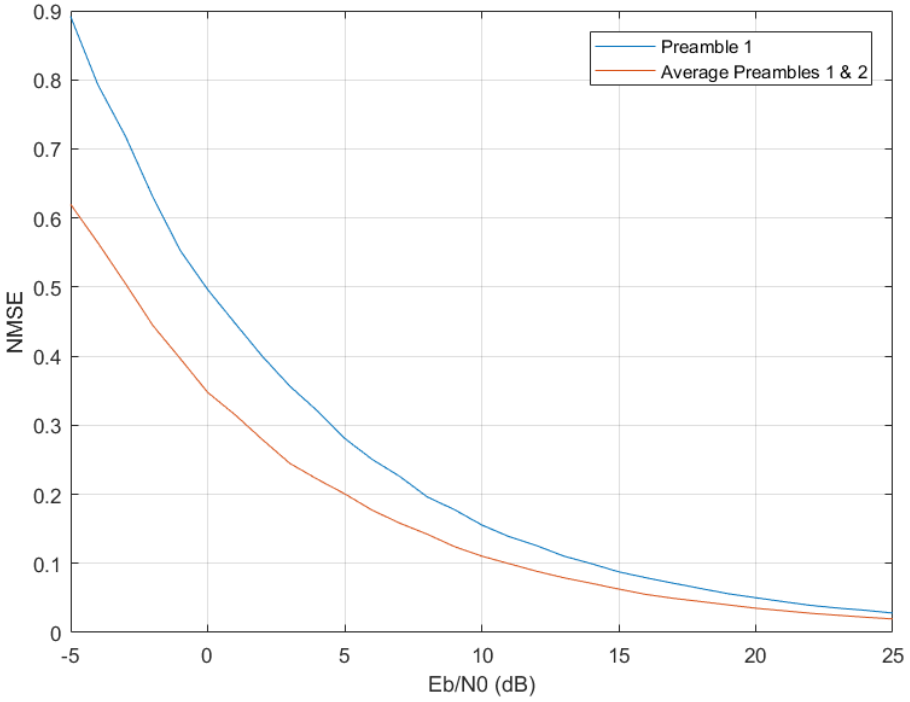

FIGURE 8 – Accuracy of the channel estimation

Figure 9 shows the degradation of the BER performance of the channel estimation, in comparison with using the true channel frequency response for the equalization task at the receiver.

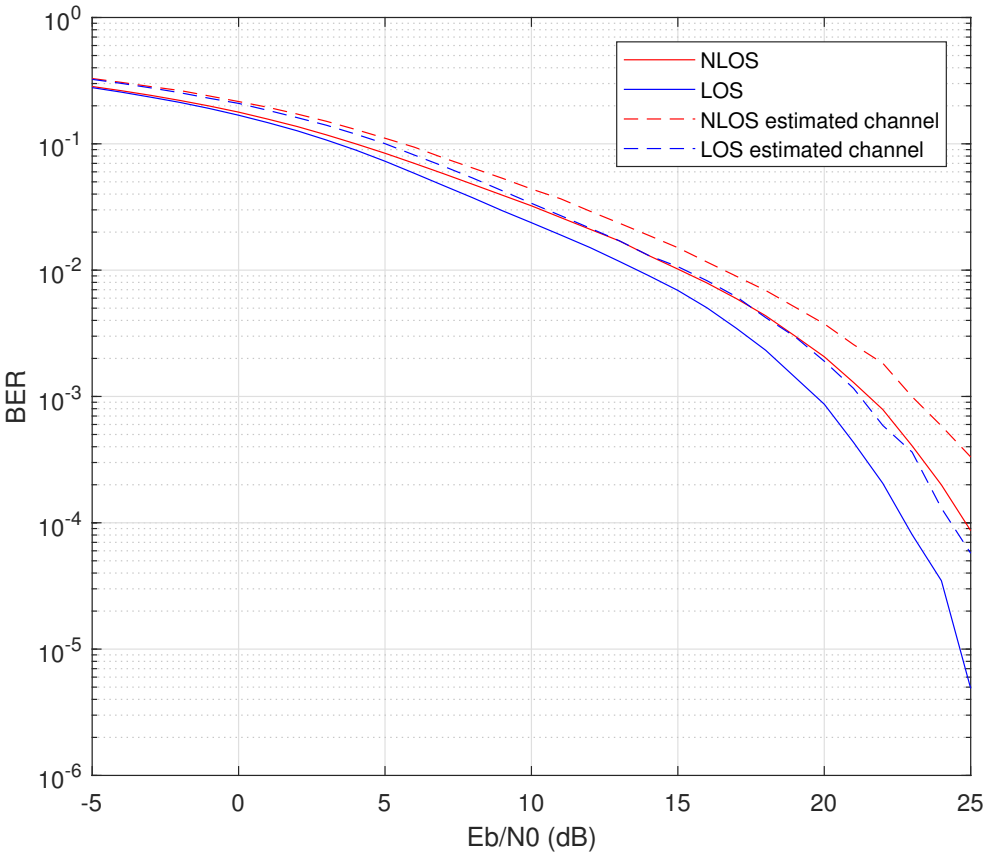

FIGURE 9 – Impact of the channel estimation on the BER performance

2.4 Synchronization

2.4.1 Time acquisition

Due to the reflections on the environment (walls, ceiling, etc.), multi path components will arrive at different time instances. It is thus important to simulate the uncertainty on the time-of-arrival (ToA) on the receiver. The ToA is added at the end of the transmitter block just before being convolved with the channel.

We simulated this uncertainty in Matlab by padding the transmitted frame with N zeros, N being a random number between 1 and 1/10 of the frame's length.

An error on the time-of-arrival estimation produces a phase rotation depending on the sub-carrier index.

2 different solutions where implemented for the time acquisition : an estimation based on the autocorrelation between successive blocks and an estimation based on the cross-correlation with the known preamble.

The maximum likelihood estimator for time n being the start of the frame is the maximum of the cross-correlation of the received sequence with preamble at time n ($C_n = \sum_{l=0}^{N-1} r_{n+l}^* a_l$)

$$\hat{n} = max_n \frac{|C_n|}{\sum_{l=0}^{N-1} |r_{n+l}|^2} \tag{13}$$

Autocorrelation between successive blocks

The first method consists of auto-correlating the signal with a version of itself delayed by a window of size N, N being the preamble size.

As the 2 preamble are repetitive, this autocorrelation will be maximum when the window is exactly at the start of the frame.

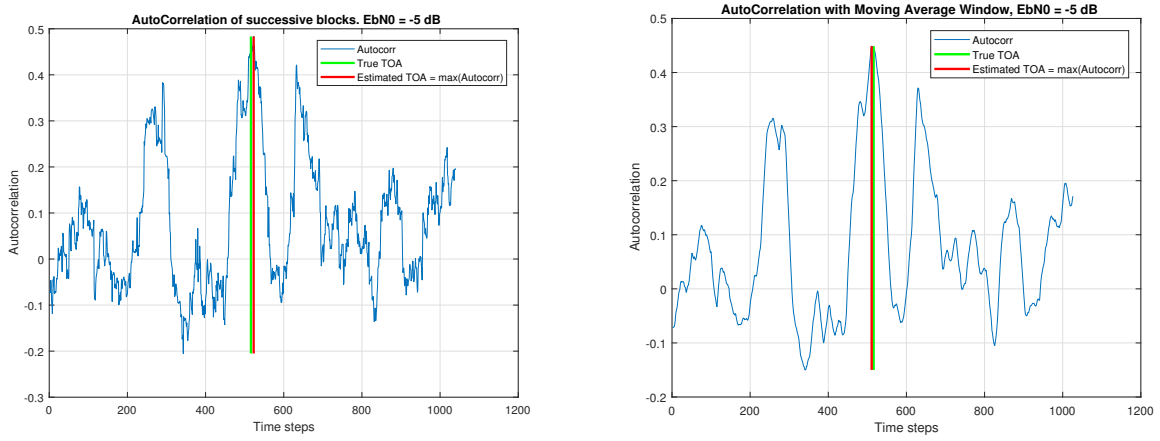

FIGURE 10 – Estimation of the Time-of-Arrival with the Autocorrelation in high noise case without and with Moving Average Window (SNR = -5 dB)

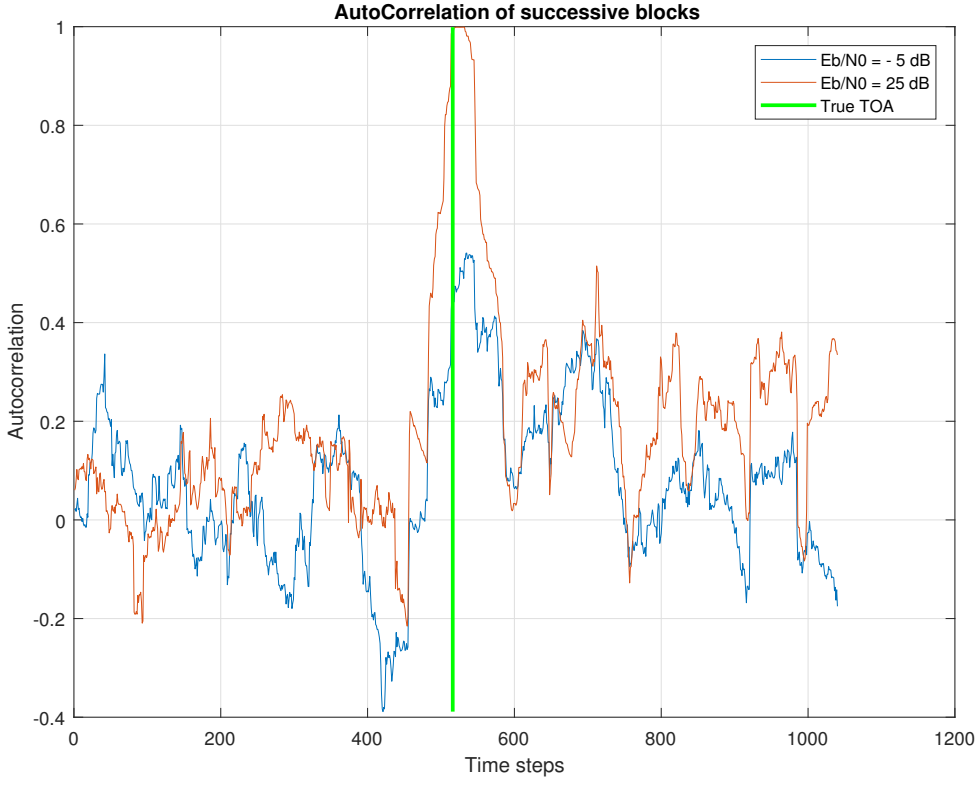

FIGURE 11 – Impact of the noise on the autocorrelation function

As expected, the magnitude of the autocorrelation is lower when the level of noise is higher. This method is robust to noise, as it is able to estimate accurately the time-of-arrival in high-noisy situations ($Eb/N0 = -5dB$).

Next, the accuracy of this method is measured with the Root Mean Square Error between the true time-of-arrival injected into the system and the estimated time-of-arrival. If there is an error on the ToA estimate, the all frame is shifted and thus the decoded bits will be erroneous.

$$RMSE = \sqrt{\frac{\sum_{k=1}^{N}(T(k) - \hat{T}(k))^2}{N}} \tag{14}$$

T being the true ToA, $\hat{T}$ the estimated ToA, N the number of experiments

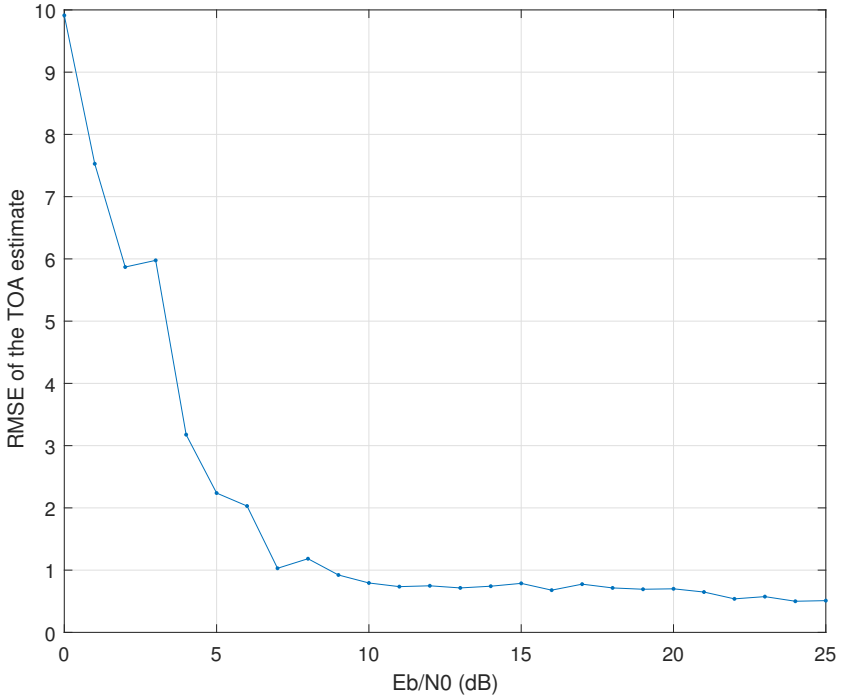

FIGURE 12 – Accuracy on the time-of-arrival estimation

Cross-correlation with preamble

This second method consists of detecting the time-of-arrival by cross-correlating the received noisy signal with the known preamble. This method is based on the fact that the receiver knows the preamble. Figure 13 shows the estimation of the time-of-arrival with the cross-correlation in high and low noise cases.

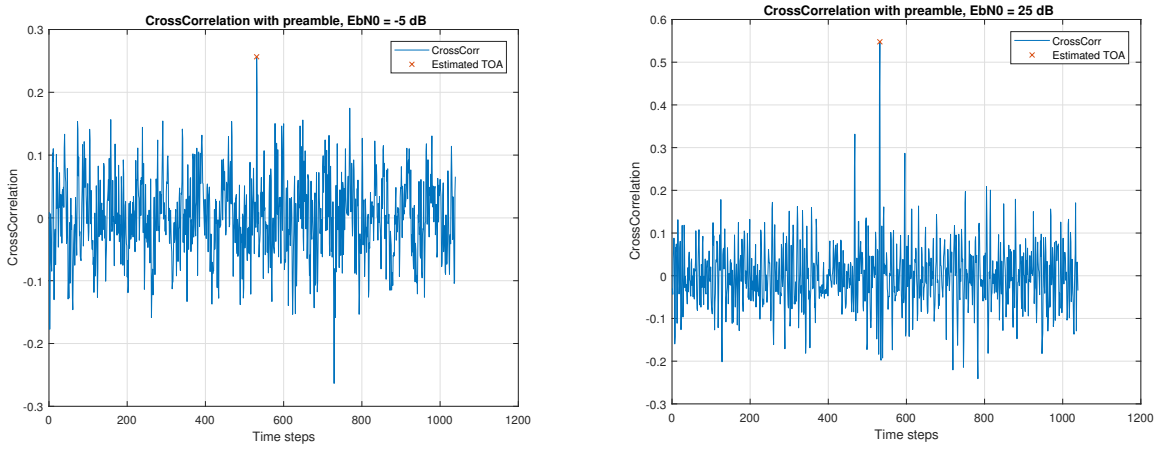

FIGURE 13 – Estimation of the time-of-arrival with cross-correlation with the known preamble in high noise (SNR = -5 dB) (a) and low noise (SNR = 25 dB) (b)

2.4.2 Frequency acquisition

Due to the difference between the local oscillators at the transmitter and receiver sides, there will be a difference in the carrier frequency (CFO).

The CFO is implemented by multiplying the transmitted signal after convolution with the channel and addition of the AWGN with a complex exponential $e^{j2\pi\Delta f}$. This will produce a progressive phase rotation and a inter-carrier interference in the frequency domain.

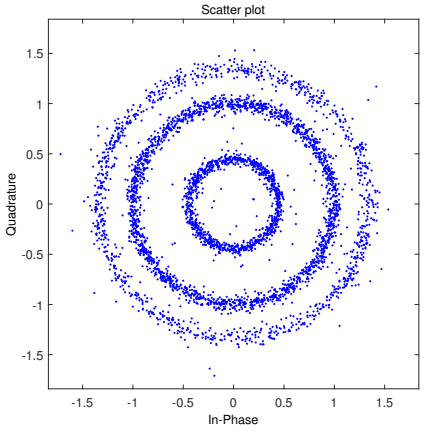

FIGURE 14 – Impact of the CFO on the transmitted symbols (16-QAM)

The CFO is compensated in 2 steps :

— At acquisition step, the constant phase shift between corresponding samples of the two repetitive preambles is removed.

— At output of acquisition, the phase shift growing is corrected with phase tracking.

Figure 15 shows the BER degradation due to the CFO estimation in the acquisition phase, for different values of CFO.

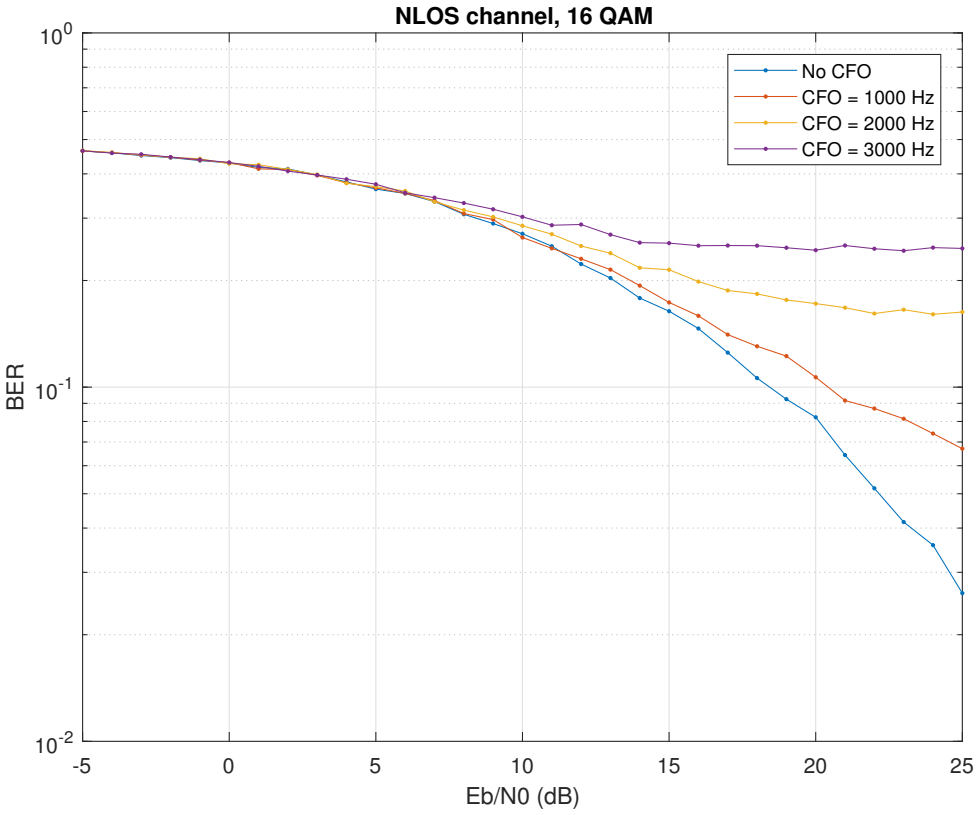

FIGURE 15 – Impact of the acquisition phase on the BER performance

An estimate of the CFO can be obtained by taking the maximum likelihood CFO estimator :

$$\hat{\Delta f} = \frac{1}{2\pi L T_s} \angle \left(\sum_{r=0}^{R-1} z_{m-r} z_{m-r-L}^{*} \right) \tag{15}$$

where z is the received continuous-time signal, rotated by a constant frequency Δf.

This phase can only be resolved in $[-\pi, \pi]$ thus the CFO can only be estimated in the range $[\frac{-1}{2LT_s}, \frac{1}{2LT_s}]Hz$. In the case where the CFO $\Delta f > \frac{1}{LT_s}$, a frequency ambiguity occurs and the CFO cannot be evaluated.

3 SIMO Communication

3.1 SIMO Channel

The channel is now going to be updated to the Single Input Multiple Output (SIMO) case by generalizing the Single Input Single Output (SISO) case. In the Narrowband :

$$y = Hx + n \tag{16}$$

where x is the symbol sent through the transmit antenna, n is the noise vector y is the vector of symbols received at the M antennas, and H the SIMO channel vector. In order to create this channel vector, the beamforming method is used.

Beamforming at the transmission side is a method that uses arrays of antennas to shape the radiation pattern and obtain constructive or destructive interferences at some specific chosen angles by controlling the phase and amplitude of the signal at each transmitting antenna. The same can be used at reception, to only receive signal from specific angles. But it can also be used at reception to compute the direction of arrival of each wave by using the beamformer function :

$$B_i(\theta,\phi) = e^{j\frac{2\pi}{\lambda}(X_i \sin(\theta)\cos(\phi)+Y_i \sin(\theta)\sin(\phi)+Z_i \cos(\theta))} \tag{17}$$

With θ and ϕ the angular direction of arrival , i the subscript of the virtual antennas and $[X_i, Y_i, Z_i]$ is the position of the i th antenna. And by knowing that the channel transfer function has the form :

$$h(t) = \sum_{i=1}^{N} a_i e^{j(\phi_i)} e^{-j(\beta_i . \vec{r})} \tag{18}$$

We can finally compute the amplitude of each incident wave in the direction (θ, ϕ) :

$$a_n(\theta,\phi) = \frac{\sum_i h_i(n).B_i^*(\theta,\phi)}{\sum_i |B_i(\theta,\phi)|^2} \tag{19}$$

The beamforming algorithm was implemented using the statistical channel transfer function of the narrowband LOS and NLOS scenario and these parameters were used :

- $\theta \in [0;\pi]$
- $\phi \in [-\pi;\pi]$
- $X, Z \in [0:9]; Y \in [9:-1:0]$
- Antenna's are spaced 2cm appart

Once the method fully implemented, the angular spectrum was computed for both NLOS and LOS scenario :

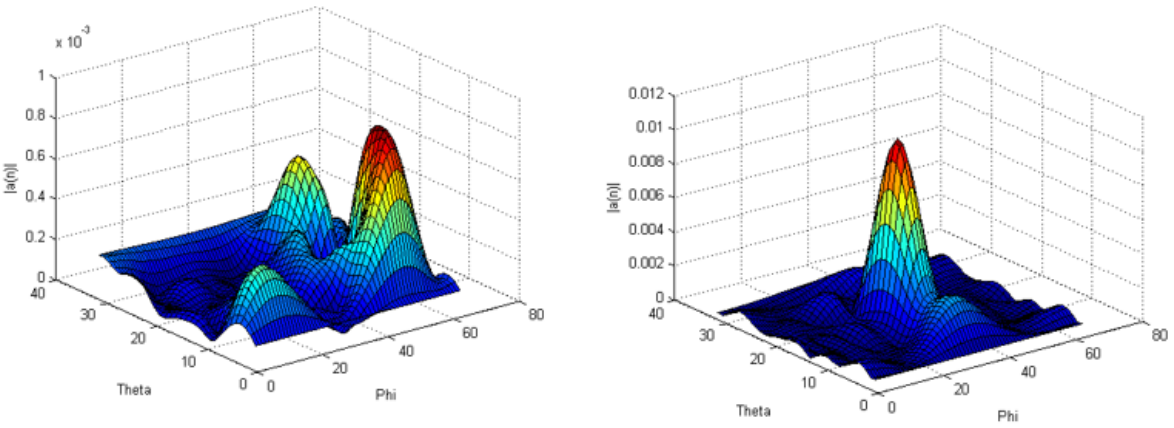

FIGURE 16 – Angular spectrum of the NLOS and LOS scenario for the 20 MHz channel

The angular spectrum for the LOS case show clearly a high peak designing the strong line of sight signal. Oppositely, The NLOS case has multiple higher peaks but still much lower than the LOS one. In order to represent the signal in the laboratory itself, two functions were used $plotImage$ and $findLocalMaxima$:

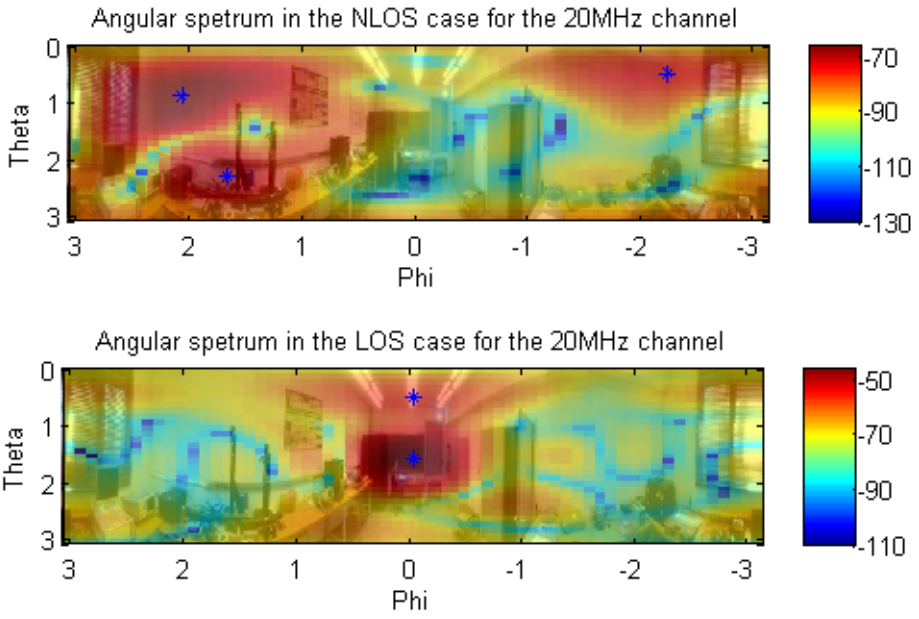

FIGURE 17 – Angular spectrum of the NLOS and LOS scenario for the 20 MHz channel

We can observe both scenario in the lab. As it can be observed on the images, the threshold for the LOS and NLOS used to find the local maxima were different as in the LOS case, there is a stronger signal.

By knowing the angular spectrum for each signal, the channel transfer function when there is multiple antennas can now be reconstruct. Indeed, at each position of an antenna, the different amplitude of each arriving wave is known and can be added together to find what each antenna is receiving. Each tap in this new channel model will be constructed from a bunch of waves according to this formula :

$$\tilde{h}_i(n) = \sum_{(\theta,\phi)} a_n(\theta,\phi) e^{j(\phi_{(\theta,\phi)} - \vec{\beta}_{(\theta,\phi)}\vec{r_i})} \tag{20}$$

With $a_n(\theta,\phi)$ is the amplitude of each wave deduced with the beamforming, $\phi_{(\theta,\phi)}$ is a random value with uniform distribution between 0 and 2π. As the statistical channel model was constructed using 10 taps, the same was applied here for both cases :

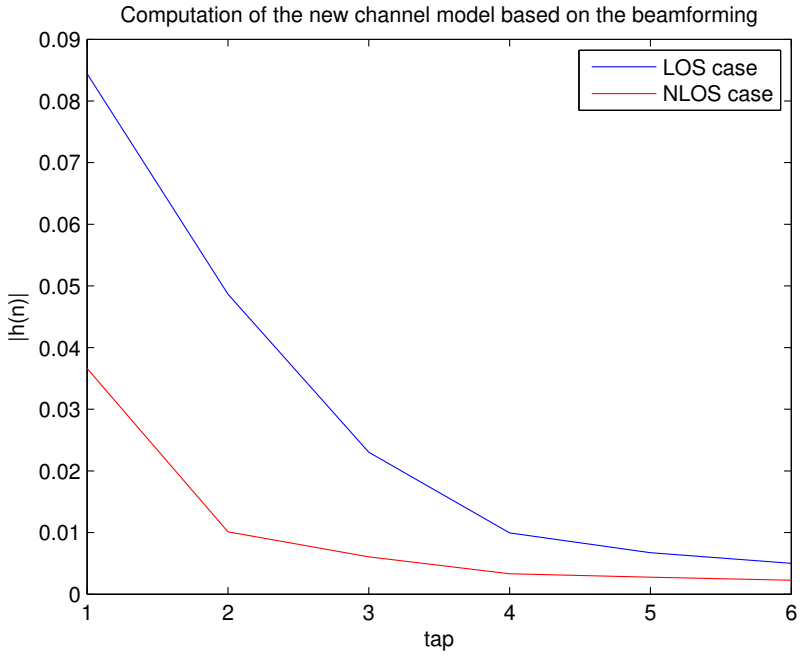

FIGURE 18 – New physical model for the channel using the beamforming method

The resulting graphs show that the LOS case has a stronger signal as expected. The next step is to study the spatial correlation of this new channel model as a function of distance between antennas, in the three directions. The wideband and narrowband cases are shown on respectively Figure 19 and Figure 20, for both LOS and NLOS. The simulation in these three direction are done using antennas separated by a 2 cm space between them. As the Clarke model represent a model where the antennas are separated by $\lambda/2$, which is approximately worth 6cm in this case, the correlation of the simulation should be higher than the correlation obtained with the Clarke model, which is consistent with the result obtained.

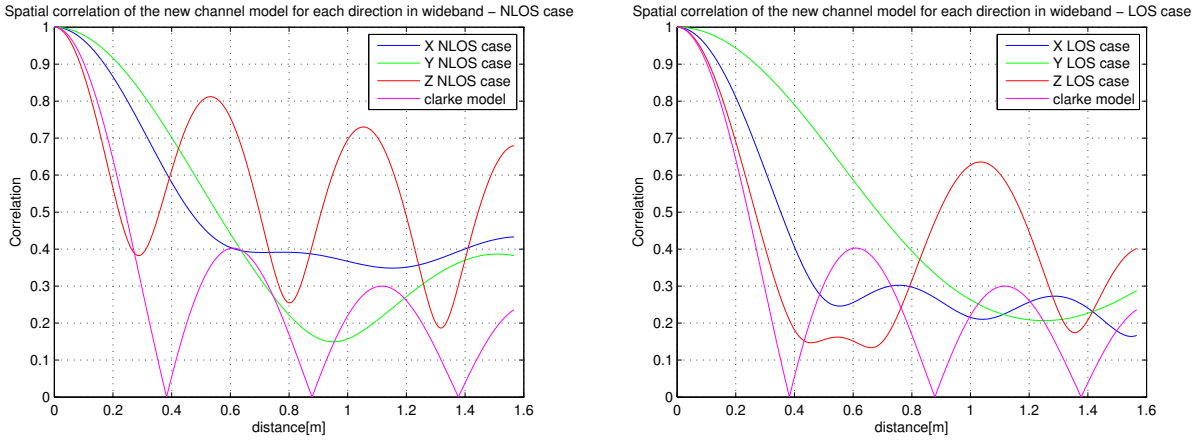

FIGURE 19 – Spatial correlation in the X,Y and Z direction for the wideband channel in the LOS case (a) NLOS case (b)

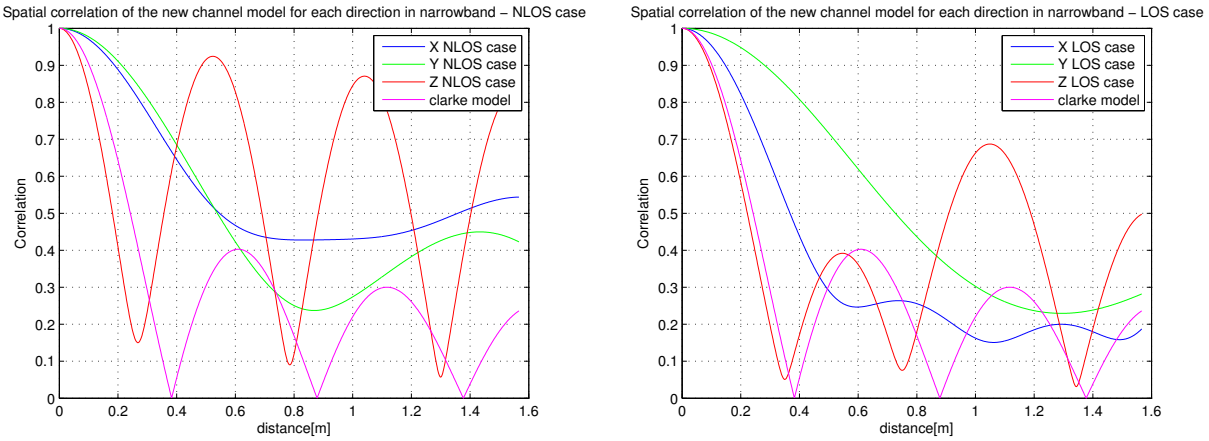

FIGURE 20 – Spatial correlation in the X,Y and Z direction for the narrowband channel in the LOS case (a) NLOS case (b)

The result for the narrowband situation should be higher than the one obtained in wideband, as the antennas cannot discrimate the MPC arriving. The results obtained in the NLOS case look more similar to the Clarke model than the ones obtained in the LOS case. This can be understood as the Clarke model represent a Rayleigh fading.

3.2 Communication with a multiple antenna receiver

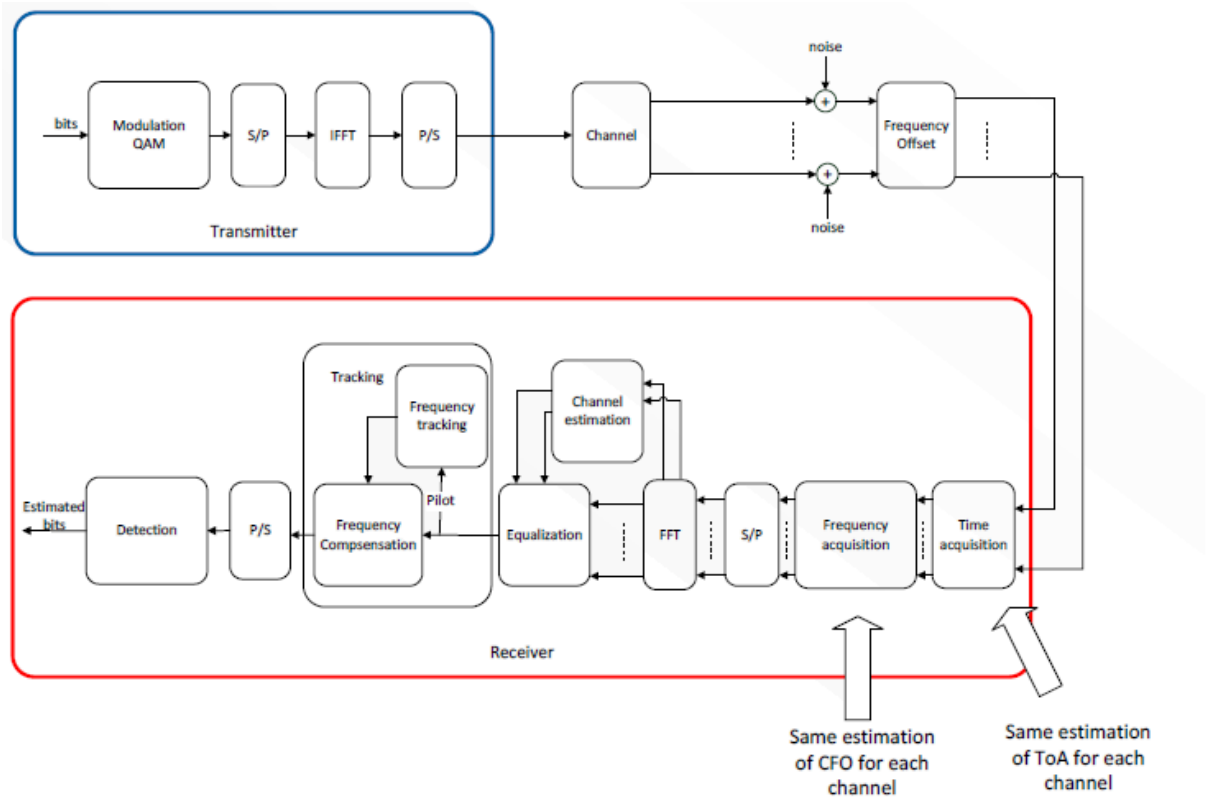

FIGURE 21 – Complete SIMO chain of communication

Using multiple antennas at the receiver allow the reception of multiple local versions. The different signals can be added together to increase the bit error rate and avoid the fading phenomenon. The chain of communication is the same as before except that this time the transmission is done over different channel to arrive at different antenna. The noise is different over each channel, but the frequency offset and the time of arrival is the same for each received signal. But as different channel are used for each antennas, the channel estimation and equalization must be done independently. For example using two receiving antennas :

$$\begin{aligned} R_1(k) &= H_1(k)S(k) + W_1(k) \\ R_2(k) &= H_2(k)S(k) + W_2(k) \end{aligned} \tag{21}$$

The independent equalized signal is :

$$\hat{S}(k) = S(k) + \frac{1}{2}\left(\frac{W_1(k)}{H_1(k)} + \frac{W_2(k)}{H_2(k)}\right) \tag{22}$$

But doing the equalization independently can create a noise amplification as shown on Figure 22.

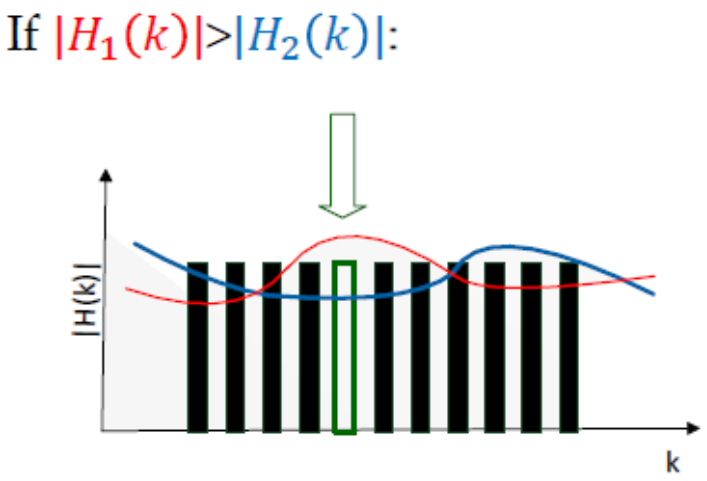

FIGURE 22 – Independent equalization

To give more importance to the channel with the higher SNR, the solution is to use the maximum ratio combining (MRC) method on each subcarrier independently. Taking back the same example, the signal equalized is :

$$\hat{S}(k) = \left(\frac{H_1'(k)R_1(k)}{|H_1(k)|^2 + |H_2(k)|^2} + \frac{H_2'(k)R_2(k)}{|H_1(k)|^2 + |H_2(k)|^2}\right) \tag{23}$$

which gives a more important weight to the more relevant information with a higher SNR.

After implementing this on Matlab, the bit error rate was assessed directly, without any CFO or time acquisition, using different numbers of antennas, to observe the effect of the SIMO system, which can be seen on Figure 23.

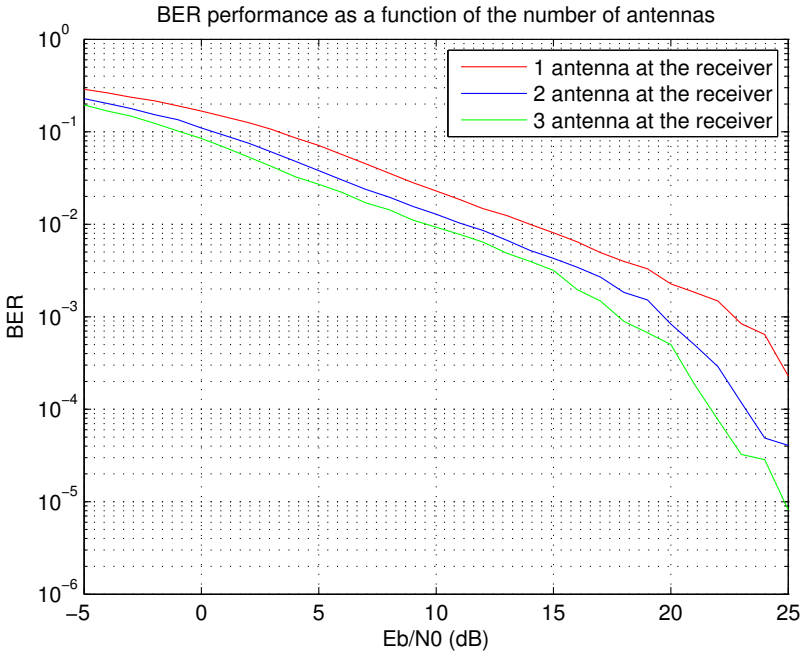

FIGURE 23 – BER using different numbers of antennas at the reception

It can be observed that as we increase the number of receiving antennas, the BER decreases. But, the number of receiving antenna is not the only thing to consider, spatial diversity of the array of antenna needs to be studied.

In order to verify that spatial diversity increase the performance of the communication chain, three cases were studied with decreasing spatial diversity, as it can be observed in Figure 24.

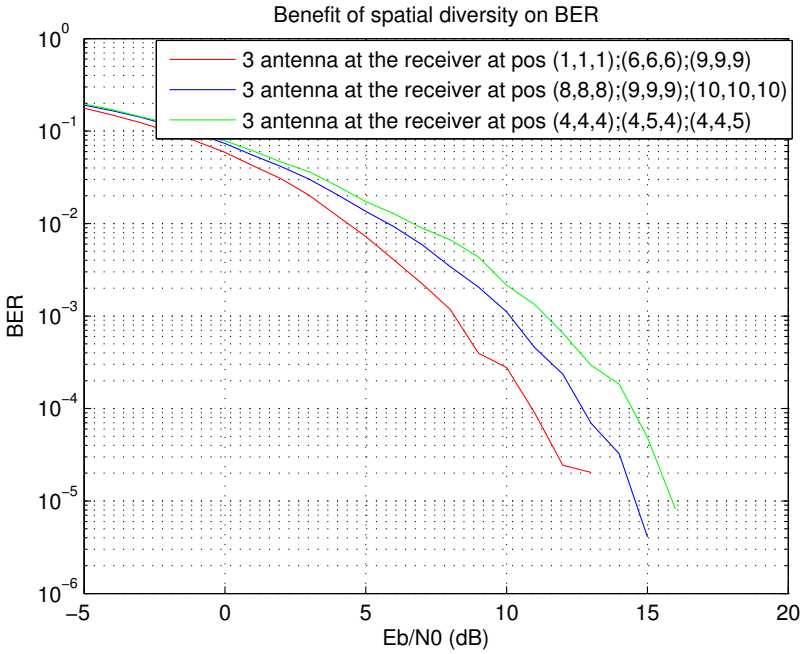

FIGURE 24 – Benefit of spatial diversity on BER curves

As expected, when the receiving antennas gets closer to each other, the performance diminish. The number of receiving antenna and their spatial diversity are both important factors.

4 Conclusion

This project was a synthesis of a important part of practical knowledges we learned during these last years. We saw once more the implementation of a wireless communication, but this time we simulated many new types of problems that we didn't experiment before, and implemented some methods to resolve them.